Passive Parameterized Time-Domain Macromodels for High-Speed Transmission-Line Networks

Pavan K. Gunupudi, *Member, IEEE,* Roni Khazaka, *Member, IEEE,* Michel S. Nakhla, *Fellow, IEEE,* Tom Smy, and Dritan Celo

***Abstract*—There is a significant need for efficient and accurate macromodels of components during the design of microwave circuits. Increased integration levels in microwave devices and higher signal speeds have produced the need to include effects previously neglected during circuit simulations. Accurate prediction of these effects involve solution of large systems of equations, the direct simulation of which is prohibitively CPU expensive.**

In this paper, an algorithm is proposed to form passive parametrized macromodels of large linear networks that match the characteristics of the original network in time, as well as other design parameters of the circuit. A novel feature of the algorithm is the ability to incorporate a set of design parameters within the reduced model. The size of the reduced models obtained using the proposed algorithm were less than 5% when compared to the original circuit. A speedup of an order of magnitude was observed for typical high-speed transmission-line networks. The algorithm is general and can be applied to other disciplines such as thermal analysis.

***Index Terms*—Macromodels and signal integrity, microwave circuits, reduced-order systems, sensitivity, transmission lines.**

I. Introduction

RAPID advances in fabrication technology have significantly reduced the feature sizes of integrated circuits (ICs) and increased the density of chips. With increasing signal speeds, transmission-line effects such as delay, coupling, reflection, and crosstalk, previously neglected during circuit simulation, have become prominent. These effects, if not predicted at early design stages, can severely degrade system performance, potentially delaying the design cycle. Accurate prediction of transmission-line effects generally requires the solution of large systems of equations, the simulation of which is prohibitively CPU expensive [1]–[3]. Forming a reduced linear model is the key to fast simulation of large transmission-line networks.

In addition to reducing the CPU expense of regular simulations, it is also important to predict the response of the designed circuit due to environmental effects, thermal effects, manufacturing variations, and fluctuations in the critical dimensions of transmission lines such as width and height. These effects induce a change in the overall system equations. It is often not feasible to perform simulation of large circuits due to variations in these parameters. A reduced-order macromodeling technique that can perform analysis on large systems of equations with respect to time and other design parameters of the circuit can aid in addressing these issues.

In the literature, several algorithms were proposed to efficiently simulate large systems of equations by model-order reduction [4]–[6]. It is to be noted that all these techniques perform model reduction with respect to a single parameter (frequency). In [7]–[9], methods have been proposed to perform multidimensional *analysis* on large systems of equations. It has to be emphasized that these techniques are *simulation* techniques and, thus, do not aid in forming time-domain macromodels. Attempts have been made to form multidimensional time-domain macromodels of linear networks in [10] and [11]. However, these techniques do not guarantee passivity of the macromodel. Passivity implies that a network cannot generate more energy than it absorbs, and no passive termination of the network will make the system unstable. Passivity is an important property because stable, but not passive, macromodels can lead to unstable or nonphysical systems when connected to other passive systems.

In this paper, a technique is proposed that can form reduced-order macromodels of large linear systems with respect to time and other design parameters of the network while guaranteeing the passivity of the reduced-order macromodel. The algorithm is based on Krylov subspace techniques extended to multiple dimensions. The theoretical approach to form passive multidimensional time-domain macromodels is presented in Section II. Proofs that the reduced-order macromodel preserves the moments of the network and conserve passivity is given is Sections III and IV, respectively. This is followed by Sections V and VI, which present the results and conclusions, respectively.

II. Multidimensional Macromodeling

A. Formulation of Network Equations

A general linear passive subnetwork, function of parameters $\lambda_1, \lambda_2, \ldots, \lambda_n$, can be expressed as

$$\mathbf{C}(\lambda_1, \ldots, \lambda_n)\frac{d\boldsymbol{x}}{dt} + \mathbf{G}(\lambda_1, \ldots, \lambda_n)\boldsymbol{x} = \mathbf{B}\boldsymbol{u_p}(t) \quad \text{(1a)}$$

$$\boldsymbol{i_p}(t) = \mathbf{B}^T\boldsymbol{x} \quad \text{(1b)}$$

where

- $\boldsymbol{x}(t, \lambda_1, \ldots, \lambda_n) \in \Re^N$ is the vector of unknowns in the system;

Manuscript received April 17, 2003. This work was supported in part by the Natural Sciences and Engineering Research Council of Canada, by Micronet, by the Gennum Corporation, and by the Center for Microelectronics Assembly and Packaging.

P. K. Gunupudi, M. S. Nakhla, T. Smy, and D. Celo are with the Department of Electronics, Carleton University, Ottawa, ON, Canada K1S 5B6 (e-mail: pavan@doe.carleton.ca; msn@doe.carleton.ca; tjs@doe.carleton.ca; dcelo@doe.carleton.ca).

R. Khazaka is with the Department of Electrical and Computer Engineering, McGill University, Montreal, QC, Canada H3A 2A7 (e-mail: roni@macs.ece.mcgill.ca).

Digital Object Identifier 10.1109/TMTT.2003.820169

- $\mathbf{C}(\lambda_1,\ldots,\lambda_n), \mathbf{G}(\lambda_1,\ldots,\lambda_n) \in \Re^{N\times N}$ are matrices describing the lumped memory and memoryless elements of the network dependent on $\lambda_1,\ldots,\lambda_n$;
- $\boldsymbol{i}_p$ and $\boldsymbol{u}_p$ denote the port currents and port voltages, respectively, p being the number of ports;
- $\mathbf{B}$ is a selector matrix that maps the port voltages into the node space of the network;
- N is the total number of variables in the MNA formulation;
- n is the number of parameters in the network.

In the remainder of this section, we shall demonstrate the inclusion of the linear subnetwork (1) into nonlinear time-domain circuit equations.

Consider a circuit ϕ containing linear and nonlinear lumped components and a linear subnetwork. The linear subnetwork is modeled using ordinary differential equations, as described in (1). Assume the network ϕ has N_ϕ nodal variables. The modified nodal analysis (MNA) matrix equations can be written in the time domain, and appended with the linear sub-circuit stamp as follows:

$$\begin{bmatrix} \mathbf{G}_\phi & \mathbf{D}\mathbf{B}^T \\ -\mathbf{B}\mathbf{D}^T & \mathbf{G} \end{bmatrix} \begin{bmatrix} \boldsymbol{x}_\phi(t) \\ \boldsymbol{x}(t) \end{bmatrix} + \begin{bmatrix} \mathbf{C}_\phi & 0 \\ 0 & \mathbf{C} \end{bmatrix} \begin{bmatrix} \dot{\boldsymbol{x}}_\phi(t) \\ \dot{\boldsymbol{x}}(t) \end{bmatrix} + \begin{bmatrix} \boldsymbol{f}_\phi(\boldsymbol{x}_\phi(t)) \\ 0 \end{bmatrix} = \begin{bmatrix} \boldsymbol{b}_\phi(t) \\ 0 \end{bmatrix} \quad (2)$$

where $\mathbf{G}_\phi \in \Re^{N_\phi\times N_\phi}$ and $\mathbf{C}_\phi \in \Re^{N_\phi\times N_\phi}$ represent the MNA matrices of the lumped elements in circuit ϕ, $\boldsymbol{f}_\phi(\boldsymbol{x}_\phi) \in \Re^{N_\phi}$, $\boldsymbol{b}_\phi(t) \in \Re^{N_\phi}$ represent the vectors of nonlinear elements and lumped sources, respectively, $\mathbf{D}_k = [d_{i,j}]$ is a selector matrix with elements $d_{i,j} \in \{0,1\}$ (where $i \in \{1,2,\ldots,N_\phi\}, j \in \{1,2,\ldots,p\}$ with a maximum of one nonzero in each row or column) that maps $\boldsymbol{v}_p(t)$ and $\boldsymbol{i}_p(t)$ into the node space $\Re^{N_\phi}$ of network ϕ.

B. Computation of the Multidimensional Subspace

The first step of the algorithm is to compute the multidimensional subspace of the system in (1). For that purpose, the block moments of $\boldsymbol{x}$ with respect to frequency (denoted by $\mathbf{Q}_s$) are computed using the procedure described in [6] and [12] using Krylov subspace techniques. Block moments of $\boldsymbol{x}$ with respect to $\lambda_1,\ldots,\lambda_n$ (denoted by matrices $\mathbf{Q}_{\lambda_i}, 1 \le i \le n$) are computed using the technique elaborated in [7]. In the special case where the variation of the matrices $\mathbf{C}$ and $\mathbf{G}$ with respect to the parameter λ_i is linear, techniques such as Arnoldi [12] can be used to compute the block moments of $\boldsymbol{x}$ with respect to λ_i to extract better efficiency. Once all the required block moments are evaluated, the multidimensional subspace (denoted by $\mathbf{Q}$) is computed such that

$$\operatorname{colsp}(\mathbf{Q}) = \operatorname{colsp}\begin{pmatrix} \mathbf{Q}_s & \mathbf{Q}_{\lambda_1} & \ldots & \mathbf{Q}_{\lambda_n} \end{pmatrix}. \quad (3)$$

This can be achieved by using a standard QR decomposition [12] on $[\mathbf{Q}_s \quad \mathbf{Q}_{\lambda_1} \quad \ldots \quad \mathbf{Q}_{\lambda_n}]$.

In the case when cross-derivatives are required to preserve the network response, the multidimensional subspace is modified to include the cross-derivatives (denoted by $\mathbf{Q}_\times$) as

$$\operatorname{colsp}(\mathbf{Q}) = \operatorname{colsp}\begin{pmatrix} \mathbf{Q_s} & \mathbf{Q_{\lambda_1}} & \ldots & \mathbf{Q_{\lambda_n}} & \mathbf{Q}_\times \end{pmatrix}. \quad (4)$$

In case the sensitivity of the moments of $\boldsymbol{x}$ with respect to a specific parameter λ_i is relatively small, the corresponding cross-derivatives can be neglected. In typical electrical subcircuits, this is generally true and it is observed that neglecting the cross-derivatives does not, in practice, effect the accuracy of the response.

It is to be noted that, once computed, the multidimensional subspace $\mathbf{Q}$ is a constant real matrix independent of frequency and $\lambda_1,\ldots,\lambda_n$.

C. Macromodeling Through Congruent Transformation

The multidimensional subspace formed in Section II-B is used to perform a congruent transformation on the original system to produce a reduced-order macromodel. Define

$$\hat{\boldsymbol{x}} = \mathbf{Q}\boldsymbol{x} \quad (5)$$

where $\hat{\boldsymbol{x}} \in \Re^q$ and $q = q_s + q_\times + \sum_{i=1}^{i=n} q_{\lambda_i}$. q_s, q_{λ_i} and $q_\times$ are the number of columns in $\mathbf{Q}_s, \mathbf{Q}_{\lambda_i}$ and $\mathbf{Q}_\times$, respectively. It has to be noted that $q \ll N$.

Using (5), a congruent transformation is performed on (1) to give

$$\hat{\mathbf{C}}(\lambda_1,\ldots,\lambda_n)\frac{d\hat{\boldsymbol{x}}}{dt} + \hat{\mathbf{G}}(\lambda_1,\ldots,\lambda_n)\hat{\boldsymbol{x}} = \hat{\mathbf{B}}\boldsymbol{u_p}(t) \quad (6a)$$

$$\boldsymbol{i_p}(t) = \hat{\mathbf{B}}^T\hat{\boldsymbol{x}} \quad (6b)$$

where

$$\hat{\mathbf{C}} = \mathbf{Q}^T\mathbf{C}\mathbf{Q} \quad \hat{\mathbf{G}} = \mathbf{Q}^T\mathbf{G}\mathbf{Q} \quad \hat{\mathbf{B}} = \mathbf{Q}^T\mathbf{B}. \quad (7)$$

It is to be noted that the size of the macromodel (6) is very small compared to the original network (1). The response at any node of the original network can be computed using (5) once the solution of the reduced system (6) is known. This reduced-order macromodel can be used in (2) instead of the original subnetwork (1).

Proof that the congruent transformation (5) preserves the first q_s and q_{λ_k} moments of $\boldsymbol{X}$ with respect to frequency and λ_k at port i is given in Section III.

III. Proof of Conservation of Moments

From (3), we have [12]

$$\begin{aligned} \operatorname{colsp}(\mathbf{Q}) &= \operatorname{colsp}\begin{pmatrix} \mathbf{Q}_s & \mathbf{Q}_{\lambda_1} & \ldots & \mathbf{Q}_{\lambda_n} \end{pmatrix} \\ &= \operatorname{colsp}\begin{pmatrix} \mathbf{M}_s & \mathbf{M}_{\lambda_1} & \ldots & \mathbf{M}_{\lambda_n} \end{pmatrix} \end{aligned} \quad (8)$$

where $\mathbf{M}_s$ are the block moments of $\boldsymbol{X}$ (the Laplace transform of $\boldsymbol{x}$) with respect to frequency and $\mathbf{M}_{\lambda_i}$ are the corresponding block moments with respect to λ_i. Hence, we have [12]

$$\mathbf{Q}\mathbf{R} = \mathbf{K} \quad (9)$$

where

$$\mathbf{K} = \begin{pmatrix} \mathbf{M}_s & \mathbf{M}_{\lambda_1} & \ldots & \mathbf{M}_{\lambda_n} \end{pmatrix}. \quad (10)$$

The reduced system in (6a) with an excitation at port i is given as

$$\hat{\mathbf{Y}}(s,\lambda_1,\ldots,\lambda_n)\hat{\mathbf{X}}(s,\lambda_1,\ldots,\lambda_n) = \hat{\boldsymbol{b}}_i \quad (11)$$

where $\hat{\mathbf{Y}}(s,\lambda_1,\ldots,\lambda_n) = \mathbf{Q}^T\mathbf{Y}(s,\lambda_1,\ldots,\lambda_n)\mathbf{Q}$, $\mathbf{Y}(s,\lambda_1,\ldots,\lambda_n) = \mathbf{G}(s,\lambda_1,\ldots,\lambda_n)+\mathbf{C}(s,\lambda_1,\ldots,\lambda_n)$, $\hat{\boldsymbol{X}}$ is the Laplace transform of $\hat{\boldsymbol{x}}$ and $\hat{\boldsymbol{b}}_i$ is the ith column of $\hat{\mathbf{B}}$. Using the congruence transformation (5), we have

$$\mathbf{Q}^T\mathbf{Y}(s,\lambda_1,\ldots,\lambda_n)\mathbf{Q}\hat{\boldsymbol{X}}(s,\lambda_1,\ldots,\lambda_n) = \mathbf{Q}^T\boldsymbol{b}_i. \quad (12)$$

Substituting (9) in (12), we have

$$\mathbf{K}^T\mathbf{Y}(s,\lambda_1,\ldots,\lambda_n)\mathbf{K}\mathbf{R}^{-1}\hat{\boldsymbol{X}}(s,\lambda_1,\ldots,\lambda_n) = \mathbf{K}^T\boldsymbol{b}_i \quad (13)$$

where $\boldsymbol{b}_i$ is the ith column of $\mathbf{B}$.

Proof that the reduced system (12) conserves q_s moments ($\mathbf{M}_s \in \Re^{N\times q_s}$) with respect to frequency is based on mathematical induction. First we prove that the zeroth moment obtained from the reduced model is equivalent to that obtained from the original system represented by (1). Next, we show that the mth moment is conserved if its previous moment is conserved.

At an expansion point $s = s_j, \lambda_1 = \lambda_1^j, \ldots, \lambda_n = \lambda_n^j$, the zeroth moment of $\boldsymbol{X}$ can be evaluated as

$$\begin{aligned}&\mathbf{K}^T\mathbf{Y}\left(s_j,\lambda_1^j,\ldots,\lambda_n^j\right)\mathbf{K}\mathbf{R}^{-1}\hat{\boldsymbol{M}}_s^0\\ &\quad= \mathbf{K}^T\boldsymbol{b}_i\\ &\quad= \mathbf{K}^T\mathbf{Y}\left(s_j,\lambda_1^j,\ldots,\lambda_n^j\right)\boldsymbol{M}_s^0\end{aligned} \quad (14)$$

where $\boldsymbol{M}_s^r$ denotes the rth moment of $\boldsymbol{X}$ with respect to frequency in the original system and $\hat{\boldsymbol{M}}_s^r$ represents the rth moment of $\hat{\boldsymbol{X}}$ with respect to frequency evaluated from the reduced system.

Since $\mathbf{K}^T\mathbf{Y}(s_j,\lambda_1^j,\ldots,\lambda_n^j)\mathbf{K}$ is nonsingular, (14) has a unique solution. Hence, $\mathbf{R}^{-1}\hat{\boldsymbol{M}}_s^0 = e_r$, where e_r is the rth column of the identity matrix $\mathbf{I}_q \in \Re^{q\times q}$ and $r = 1$ represents a unique solution of (14). Next, from (5), the zeroth moment of $\boldsymbol{X}(s,\lambda_1,\ldots,\lambda_n)$ is obtained as

$$\mathbf{Q}\hat{\boldsymbol{M}}_s^0 = \mathbf{K}\mathbf{R}^{-1}\hat{\boldsymbol{M}}_s^0 = \mathbf{K}e_r = \boldsymbol{M}_s^0. \quad (15)$$

Here, as seen from the right-hand side (RHS) of (15), the zeroth moment of the system is conserved.

We now proceed to prove that if the hypothesis holds well for $l = m-1$, i.e., $\mathbf{Q}\hat{\boldsymbol{M}}_s^l = \boldsymbol{M}_s^l$, then it also holds well for $l = m$, i.e., $\mathbf{Q}\hat{\boldsymbol{M}}_s^m = \boldsymbol{M}_s^m$.

The mth moment of $\hat{\boldsymbol{X}}(s,\lambda_1,\ldots,\lambda_n)$ with respect to frequency can be evaluated [5] and simplified using (13) as

$$\mathbf{K}^T\mathbf{Y}\left(s_j,\lambda_1^j,\ldots,\lambda_n^j\right)\mathbf{K}\mathbf{R}^{-1}\hat{\boldsymbol{M}}_s^m = -\mathbf{K}^T\frac{\partial\mathbf{Y}}{\partial s}\mathbf{K}\mathbf{R}^{-1}\hat{\boldsymbol{M}}_s^{m-1}. \quad (16)$$

Since the hypothesis holds well for $l = m-1, \mathbf{R}^{-1}\hat{\boldsymbol{M}}_s^{m-1} = e_r$, where r corresponds to the location of $\boldsymbol{M}_s^{m-1}$ in $\mathbf{K}$. This reduces (16) to

$$\begin{aligned}&\mathbf{K}^T\mathbf{Y}\left(s_j,\lambda_1^j,\ldots,\lambda_n^j\right)\mathbf{K}\mathbf{R}^{-1}\hat{\boldsymbol{M}}_s^m\\ &\quad= -\mathbf{K}^T\frac{\partial\mathbf{Y}}{\partial s}\boldsymbol{M}_s^{m-1}\\ &\quad= \mathbf{K}^T\mathbf{Y}\left(s_j,\lambda_1^j,\ldots,\lambda_n^j\right)\boldsymbol{M}_s^m.\end{aligned} \quad (17)$$

Again, since $\mathbf{K}^T\mathbf{Y}(s_j,\lambda_1^j,\ldots,\lambda_n^j)\mathbf{K}$ is nonsingular, (17) has a unique solution. Hence, $\mathbf{R}^{-1}\hat{\boldsymbol{M}}_s^m = e_r$, where r corresponds to the location of $\boldsymbol{M}_s^m$ in $\mathbf{K}$, and represents the unique solution for (17). Next, from (5), the mth moment of $\boldsymbol{X}(s,\lambda)$ is obtained as

$$\mathbf{Q}\hat{\boldsymbol{M}}_s^m = \mathbf{K}\mathbf{R}^{-1}\hat{\boldsymbol{M}}_s^m = \mathbf{K}e_r = \boldsymbol{M}_s^m. \quad (18)$$

Hence, the mth moment of the system with respect to frequency is conserved if the previous moment is conserved. Thus, by *mathematical induction*, we can conclude that q_s moments of $\mathbf{Q}\hat{\boldsymbol{X}}(s,\lambda_1,\ldots,\lambda_n) = \mathbf{Q}\hat{\mathbf{Y}}^{-1}(s,\lambda_1,\ldots,\lambda_n)\hat{\boldsymbol{b}}_i$ are the same as q_s moments of $\boldsymbol{X}(s,\lambda_1,\ldots,\lambda_n) = \mathbf{Y}^{-1}(s,\lambda_1,\ldots,\lambda_n)\boldsymbol{b}_i$

Similarly, we proceed with the proof that the reduced system (12) conserves q_{λ_k} moments ($\mathbf{M}_{\lambda_k} \in \Re^{N\times q_{\lambda_k}}$) with respect to λ_k. The proof that the zeroth moment obtained from the reduced model is equivalent to that obtained from the original system represented by (1) has already been proven above. We now show that the mth moment is conserved if all the previous moments are conserved, i.e., if the hypothesis holds well for $0 \le l \le m-1$, i.e., $\mathbf{Q}\hat{\boldsymbol{M}}_{\lambda_k}^l = \boldsymbol{M}_{\lambda_k}^l$, then it also holds well for $l = m$, i.e., $\mathbf{Q}\hat{\boldsymbol{M}}_{\lambda_k}^m = \boldsymbol{M}_{\lambda_k}^m$.

The mth moment of $\boldsymbol{X}(s,\lambda_1,\ldots,\lambda_n)$ with respect to λ_k can be evaluated [5] and simplified using (13) as

$$\begin{aligned}&\mathbf{K}^T\mathbf{Y}(s_j,\lambda_1^j,\ldots,\lambda_n^j)\mathbf{K}\mathbf{R}^{-1}\hat{\boldsymbol{M}}_{\lambda_k}^m\\ &\qquad= -\sum_{q=1}^{m}\frac{\mathbf{K}^T\left[\dfrac{\partial^q\mathbf{Y}}{\partial\lambda_k^q}\right]\mathbf{K}\mathbf{R}^{-1}\hat{\boldsymbol{M}}_{\lambda_k}^{m-q}}{q!}.\end{aligned} \quad (19)$$

Since the hypothesis holds well for all $0 \le l \le m-1$, $\mathbf{R}^{-1}\hat{\boldsymbol{M}}_{\lambda_k}^l = e_r$, where r corresponds to the location of $\boldsymbol{M}_{\lambda_k}^l$ in $\mathbf{K}$. This reduces (19) to

$$\begin{aligned}&\mathbf{K}^T\mathbf{Y}\left(s_j,\lambda_1^j,\ldots,\lambda_n^j\right)\mathbf{K}\mathbf{R}^{-1}\hat{\boldsymbol{M}}_{\lambda_k}^m\\ &\quad= -\sum_{q=1}^{m}\frac{\mathbf{K}^T\left[\dfrac{\partial^q\mathbf{Y}}{\partial\lambda_k^q}\right]\mathbf{K}\mathbf{R}^{-1}\boldsymbol{M}_{\lambda_k}^{m-q}}{q!}\\ &\quad= \mathbf{K}^T\mathbf{Y}\left(s_j,\lambda_1^j,\ldots,\lambda_n^j\right)\boldsymbol{M}_{\lambda_k}^m.\end{aligned} \quad (20)$$

Again, since $\mathbf{K}^T\mathbf{Y}(s_j,\lambda_1^j,\ldots,\lambda_n^j)\mathbf{K}$ is nonsingular, (19) has a unique solution. Hence, $\mathbf{R}^{-1}\hat{\boldsymbol{M}}_{\lambda_k}^m = e_r$, where r corresponds to the location of $\boldsymbol{M}_{\lambda_k}^m$ in $\mathbf{K}$, and represents the unique solution for (19). Next, from (5), the mth moment of $\boldsymbol{X}(s,\lambda)$ is obtained as

$$\mathbf{Q}\hat{\boldsymbol{M}}_{\lambda_k}^m = \mathbf{K}\mathbf{R}^{-1}\hat{\boldsymbol{M}}_{\lambda_k}^m = \mathbf{K}e_r = \boldsymbol{M}_{\lambda_k}^m. \quad (21)$$

Hence, the mth moment of the system with respect to λ_k is conserved if all the previous moments are conserved. Thus, by *mathematical induction*, we can conclude that q_{λ_k} moments of $\mathbf{Q}\hat{\boldsymbol{X}}(s,\lambda_1,\ldots,\lambda_n) = \mathbf{Q}\hat{\mathbf{Y}}^{-1}(s,\lambda_1,\ldots,\lambda_n)\hat{\boldsymbol{b}}_i$ are the same as q_{λ_k} moments of $\boldsymbol{X}(s,\lambda_1,\ldots,\lambda_n) = \mathbf{Y}^{-1}(s,\lambda_1,\ldots,\lambda_n)\boldsymbol{b}_i$.

IV. Proof of Passivity

Passivity implies that a network cannot generate more energy than it absorbs, and no passive termination of the network will make the system unstable. Passivity is an important property because stable, but not passive, macromodels can lead to unstable systems when connected to other passive systems. A network is passive iff its admittance (or impedance) parameter matrix is positive real. The necessary and sufficient conditions for the network admittance matrix $\mathbf{H}(s) = \hat{\mathbf{B}}^T\{\hat{\mathbf{G}} + s\hat{\mathbf{C}}\}^{-1}\hat{\mathbf{B}}$ to be passive are the following:

- $\mathbf{H}(s^*) = \mathbf{H}^*(s)$ for all complex s, where $*$ is the complex conjugate operator;
- $\mathbf{H}(s)$ is positive real, i.e., $z^{*T}\{\mathbf{H}(s)+\mathbf{H}^T(s^*)\}z \geq 0$ for all complex values of s satisfying $\mathrm{Re}(s) \geq 0$ and for any complex vector z.

Verifying condition 1 for the admittance matrix obtained from the reduced order system, we have

$$\begin{aligned}\mathbf{H}(s^*) &= \hat{\mathbf{B}}^T\{\hat{\mathbf{G}} + s^*\hat{\mathbf{C}}\}^{-1}\hat{\mathbf{B}} \\ &= \hat{\mathbf{B}}^T\left\{\left(\hat{\mathbf{G}} + s\hat{\mathbf{C}}\right)^{-1}\right\}^*\hat{\mathbf{B}} \\ &= \mathbf{H}^*(s). \end{aligned} \tag{22}$$

Hence, condition 1 is satisfied. Now, we have

$$\begin{aligned} & z^{*T}\left\{\mathbf{H}(s) + \mathbf{H}^T(s^*)\right\}z \\ &\quad = z^{*T}\left[\hat{\mathbf{B}}^T\{\hat{\mathbf{G}} + s\hat{\mathbf{C}}\}^{-1}\hat{\mathbf{B}} + \hat{\mathbf{B}}^T\{\hat{\mathbf{G}} + s^*\hat{\mathbf{C}}\}^{-T}\hat{\mathbf{B}}\right]z \\ &\quad = z^{*T}\hat{\mathbf{B}}^T\{\hat{\mathbf{G}} + s\hat{\mathbf{C}}\}^{-1}\left[\hat{\mathbf{G}} + s\hat{\mathbf{C}} + \{\hat{\mathbf{G}} + s^*\hat{\mathbf{C}}\}^T\right] \\ &\qquad \times \{\hat{\mathbf{G}} + s^*\hat{\mathbf{C}}\}^{-T}\hat{\mathbf{B}}z. \end{aligned} \tag{23}$$

Letting $w = \{\hat{\mathbf{G}} + s^*\hat{\mathbf{C}}\}^{-T}\hat{\mathbf{B}}z$ (23) reduces to

$$\begin{aligned} & z^{*T}\left\{\mathbf{H}(s) + \mathbf{H}^T(s^*)\right\}z \\ &\qquad = w^{*T}\left[\{\hat{\mathbf{G}} + s\hat{\mathbf{C}}\} + \{\hat{\mathbf{G}} + s^*\hat{\mathbf{C}}\}^T\right]w \end{aligned} \tag{24}$$

The term on the RHS of (24) has been proven to be nonnegative in [6] provided $\mathbf{G}(s, \lambda_1, \ldots, \lambda_n)$ and $\mathbf{C}(s, \lambda_1, \ldots, \lambda_n)$ are nonnegative definite (i.e., the original network (1) is passive). Hence, we can say that

$$z^{*T}\{\mathbf{H}(s) + \mathbf{H}^T(s^*)\}z \geq 0. \tag{25}$$

Thus, the system admittance matrix derived from the reduced-order model satisfies condition 2. Consequently, we can conclude that the system is passive. It is to be noted that, in this proof, no assumption on the transformation matrix $\mathbf{Q}$ has been made other than the fact that it is a real matrix.

V. Results

A. Example 1

A distributed transmission-line network with two input/output ports containing a set of nine coupled transmission lines [13] and *RLC* components was chosen to demonstrate the efficiency and accuracy of the proposed algorithm. The distributed network was discretized using lumped segmentation. The size of the MNA equations representing this network was 3612×3612. The proposed algorithm can be used to form a macromodel of the distributed network as a function of time/frequency and any design parameter of the network. For this specific example, the length of the transmission line was taken as the design parameter of interest. Block moments with respect to frequency, as well as the length of the transmission lines were considered to form the reduced-order macromodel. The size of the equations representing the reduced macromodel was 150×150. The CPU cost of performing the reduction was 21.43 s. Note that this is a one-time cost to form the reduced model and does not need to be repeated for each new frequency point or line length. A comparison of the Y-parameters of the original network and the reduced macromodel are shown in Fig. 1(a) and (b). The Y-parameters obtained from the reduced macromodel match the results of the original system accurately

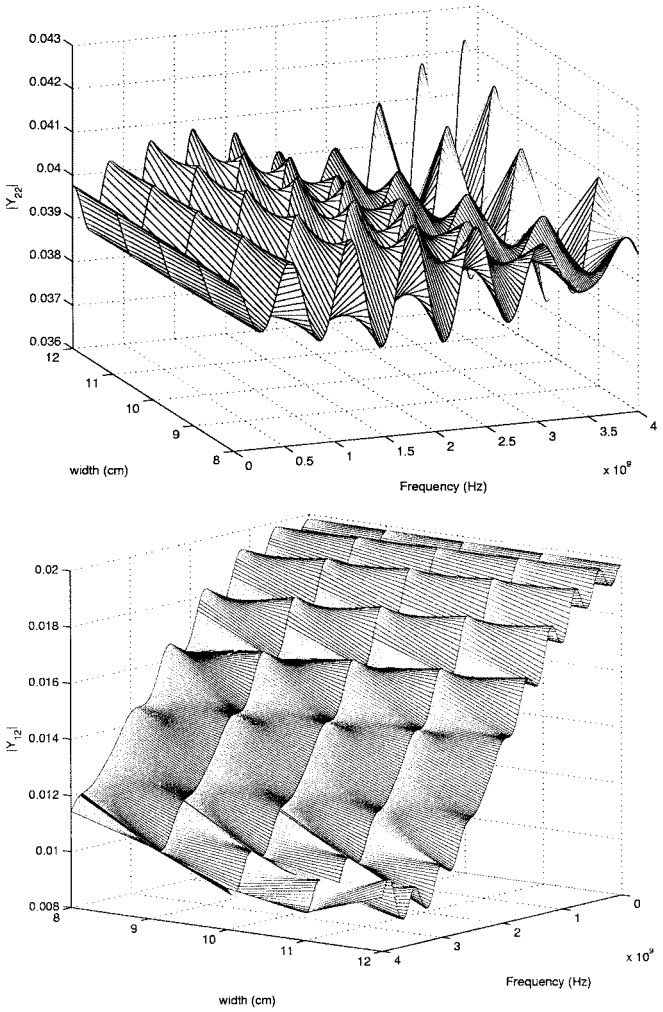

Fig. 1. $|Y_{22}|$ and $|Y_{12}|$ of the macromodel in example 1 are shown as the length of transmission line is varied from 8 to 12 cm. The results from the reduced macromodel are within 0.26% of the values obtained from the full simulation and, hence, the surfaces are not visually distinguishable.

TABLE I
CPU Comparison for Example 1

	Size	Sim. Time	Speed-up
Org. System	3612 × 3612	2916s	–
Red. System	150 × 150	254s	11.48

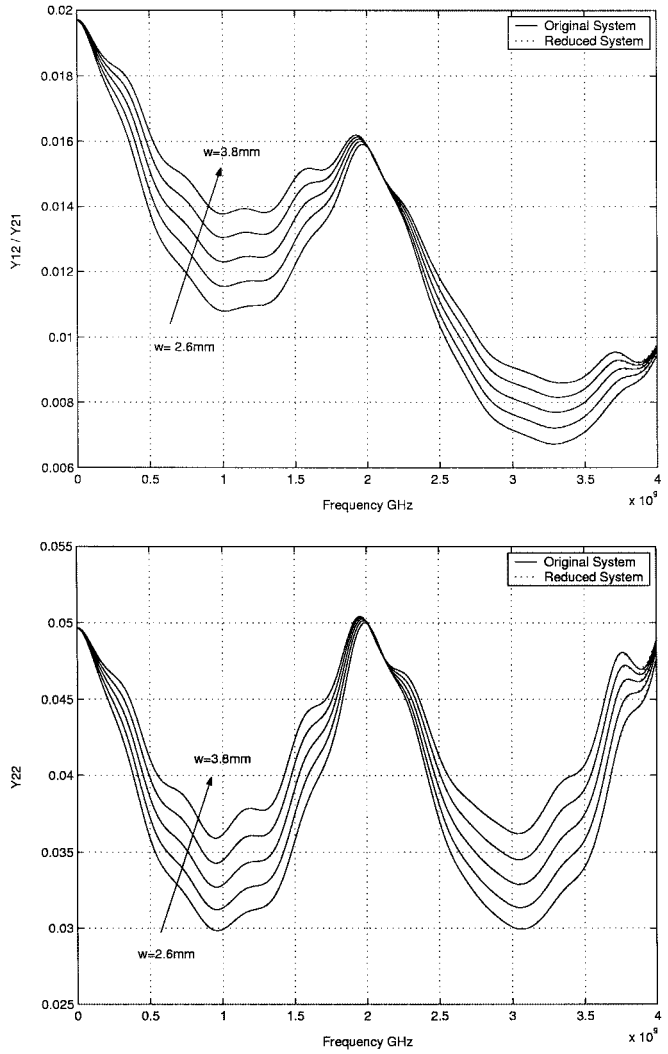

Fig. 2. $|Y_{12}|$ and $|Y_{22}|$ obtained from the reduced-order macromodel are compared with the responses from the original system in example 2 as the width of transmission lines are varied from 2.6 to 3.8 mm.

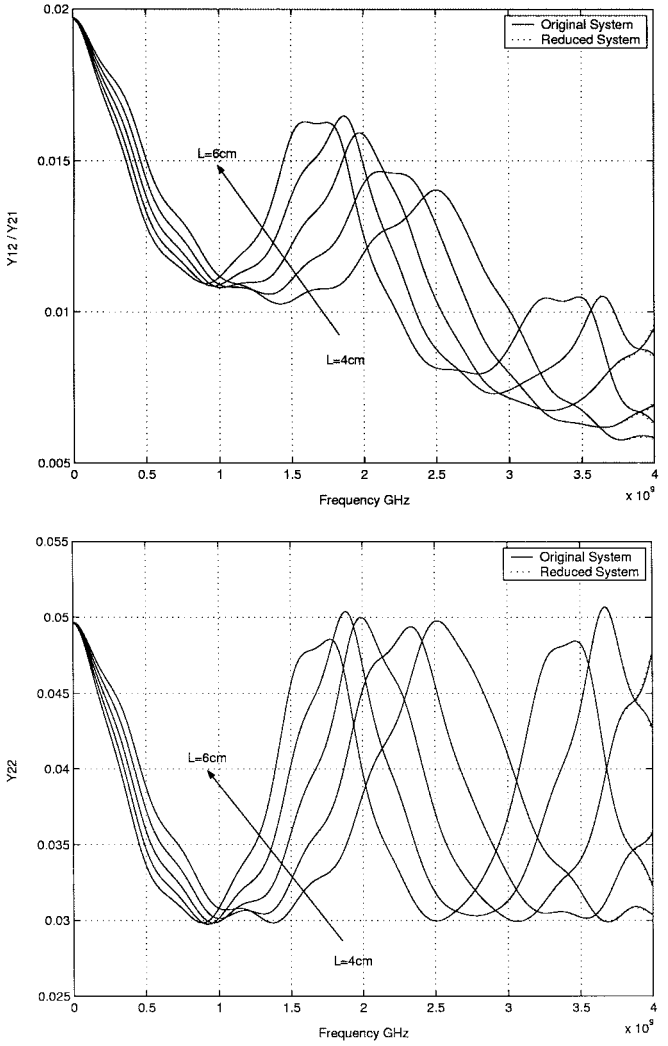

Fig. 3. $|Y_{12}|$ and $|Y_{22}|$ obtained from the reduced-order macromodel are compared with the responses from the original system in example 2 as the length of the transmission lines are varied from 4 to 6 cm.

TABLE II
CPU COMPARISON FOR EXAMPLE 2—FREQUENCY-DOMAIN ANALYSIS

Original System Size = 3552	Reduced System Size	Reduction Time	Org. Sim. Time	Red. Sim. Time	Mean Error	Speed-up
Freq. and width	218	27.23s	947.9s	25.12s	0.03%	38
Freq. and length	228	26.9s	972s	27.8s	0.04%	35
Freq., width and length	246	28.4s	4726s	150.5s	0.022%	31

(error within 0.26%). For this analysis, 512 frequency points were taken at nine different values of the line length ranging from 8 to 12 cm. A comparison of the CPU time taken to generate the responses in Fig. 1 is shown in Table I. A speed up of 11.48 was achieved using the proposed algorithm.

B. Example 2

A two-port network consisting of 18 transmission lines and *RLC* components is considered for this example. The distributed elements in the network were discretized using lumped segmentation. The size of the MNA matrices was 3552×3552. The proposed algorithm was used to perform an analysis on this network by varying the width and length of the transmission lines. In order to demonstrate the accuracy and efficiency of the proposed algorithm, three different macromodels of the transmisson-linenetwork were generated that model the behavior of the original network with respect to different parameters.

The first macromodel was formed using the proposed algorithm to model variations with respect to frequency and width of the transmission lines. One hundred moments with respect to frequency and five moments with respect to width along with four cross moments were used to generate the reduced-order macromodel. The size of the reduced model was 218×218. A comparison of the frequency response obtained from the original system and the reduced-order macromodel is shown in Fig. 2. The mean error in the response of the reduced-order macromodel when compared to the original network was found to be 0.03%. A comparison of CPU times taken to perform the analysis is shown in Table II. As we can see, a speed-up of 38 was obtained for frequency-domain analysis by using the proposed algorithm.

The second macromodel was formed using the proposed algorithm to model variations with respect to frequency and length of the transmission lines. One hundred moments with respect to frequency and ten moments with respect to length along with

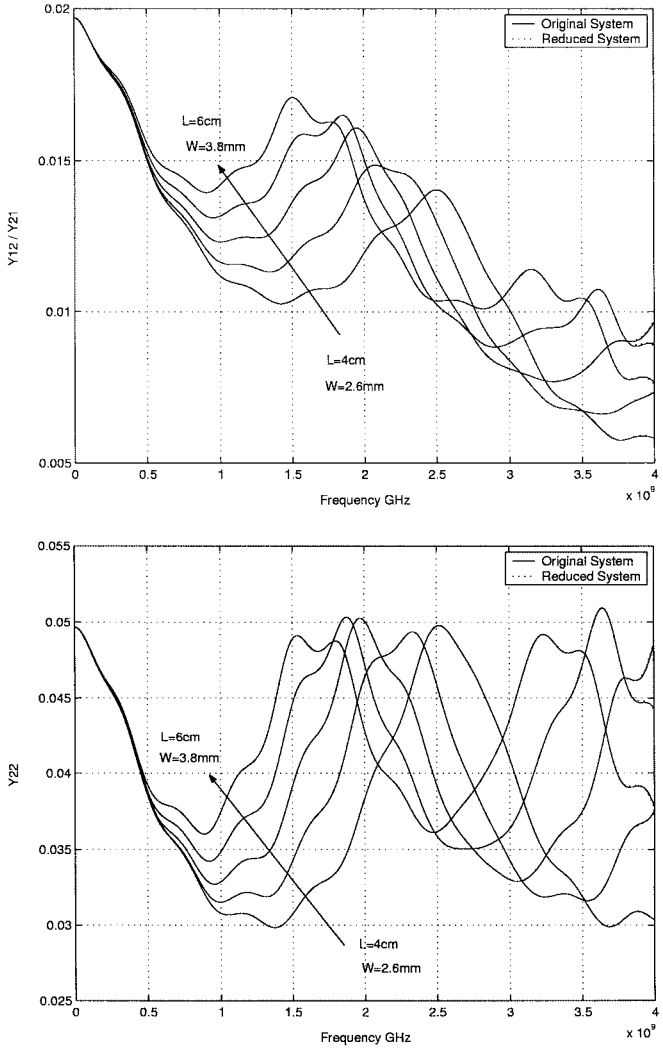

Fig. 4. $|Y_{12}|$ and $|Y_{22}|$ obtained from the reduced-order macromodel are compared with the responses from the original system in example 2 as the width of the transmission lines is varied from 2.6 to 3.8 mm and the length is changed from 4 to 6 cm.

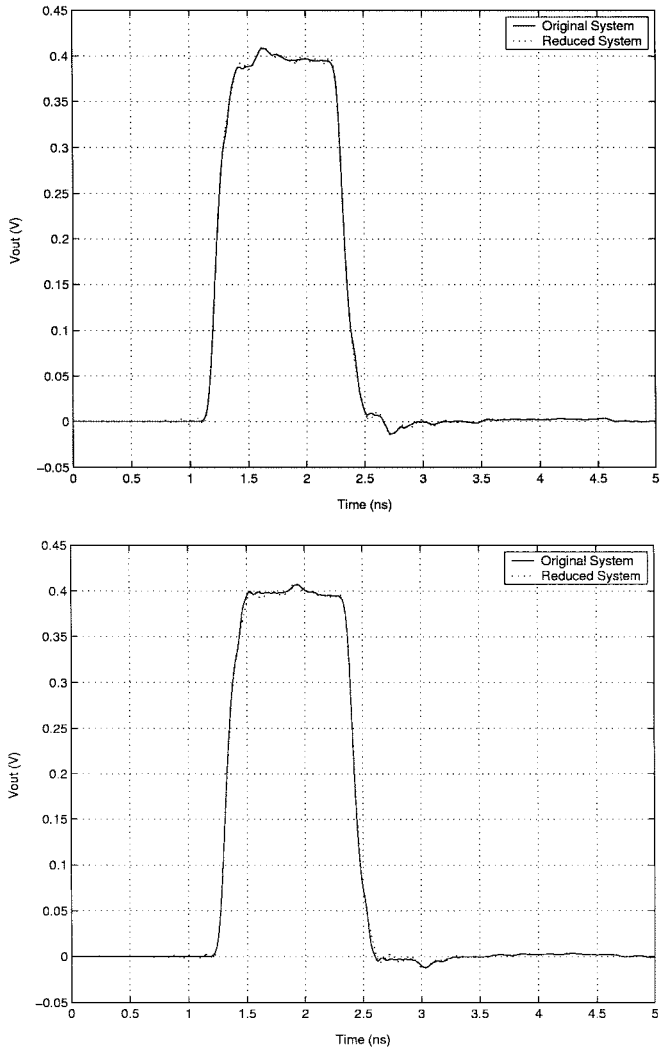

Fig. 5. Comparison of the transient results obtained from the reduced-order macromodel and the original system in example 2 by driving with a 1-V pulse with a rise/fall time of 0.1 ns and a pulsewidth of 1 ns.

four cross moments were used to form the reduced-order macromodel. The size of the reduced model was 228×228. The frequency responses obtained from the original and reduced systems are compared in Fig. 3. The mean error in the response of the reduced-order macromodel when compared to the original network was found to be 0.04%. As we can see from the CPU comparison in Table II, a speed-up of 35 was achieved using the proposed algorithm.

The proposed algorithm was used to generate a third macromodel to model variations with respect to frequency, length, and width of the transmission lines. One hundred moments with respect to frequency, five moments with respect to width, and ten moments with respect to length along with eight cross moments were used to form the reduced-order macromodel. The size of the reduced model was 246×246. A comparison of the frequency response obtained from the original system and the reduced-order macromodel is shown in Fig. 4. The mean error in the response of the reduced-order macromodel when compared to the original network was found to be 0.022%. As we can see from the CPU comparison in Table II, a speed-up of 31 was achieved using the proposed algorithm. Transient results are shown in Fig. 5. CPU results for the transient analysis are shown in Table III, indicating a speed-up of 13 with respect to the solution obtained from the original circuit.

TABLE III
CPU COMPARISON FOR EXAMPLE 2—TRANSIENT ANALYSIS FOR WIDTH $= 2.6$ mm AND LENGTH $= 4$ cm

	Size	Sim. Time	Speed-up
Org. System	3552	223s	–
Red. System	226	16s	14

VI. CONCLUSION

This paper has presented an new technique that forms reduced-order macromodels, which model the original network with respect to time, as well as multiple design parameters. The proposed algorithm was tested on several large networks to form multidimensional macromodels. The size of the reduced models were less than 5% when compared to the original circuit.

REFERENCES

[1] M. Nakhla and R. Achar, *Handbook on VLSI*. Boca Raton, FL: CRC, 2000, ch. Modeling and Simulation of High-Speed Interconnects.

[2] A. Deutsch, "Electrical characteristics of interconnects for high-performance systems," *Proc. IEEE*, vol. 86, pp. 315–355, Feb. 1998.

[3] C. Paul, *Analysis of Multiconductor Transmission Lines*. New York: Wiley, 1994.

[4] L. T. Pileggi and R. A. Roher, "Asymptotic waveform evaluation for timing analysis," *IEEE Trans. Computer-Aided Design*, vol. 9, pp. 352–366, Apr. 1990.

[5] E. Chiprout and M. S. Nakhla, "Analysis of interconnect networks using complex frequency hopping (CFH)," *IEEE Trans. Computer-Aided Design*, vol. 14, pp. 186–200, Feb. 1995.

[6] A. Odabasioglu, M. Celik, and L. T. Pileggi, "Prima: Passive reduced-order interconnect macromodeling algorithm," *IEEE Trans. Computer-Aided Design*, vol. 17, pp. 645–653, Aug. 1998.

[7] P. Gunupudi and M. Nakhla, "Multi-dimensional model reduction of VLSI interconnects," in *Proc. IEEE Custom Integrated Circuits Conf.*, May 2000, pp. 499–502.

[8] P. Gunupudi, R. Khazaka, and M. S. Nakhla, "Analysis of transmission line circuits using multi-dimensional model reduction techniques," in *Proc. IEEE Topical Electrical Performance on Electronic Packaging Meeting*, Boston, MA, Oct. 2001, pp. 43–46.

[9] P. Gunupudi, R. Khazaka, and M. Nakhla, "Analysis of transmission line circuits using multi-dimensional model reduction techniques," *IEEE Trans. Adv. Packag.*, vol. 25, pp. 174–180, May 2002.

[10] E. Acar, S. Nassif, Y. Liu, and L. T. Pillegi, "Time-domain simulation of variational interconnect models," in *Int. Quality Electronic Design Symp.*, San Jose, CA, Mar. 2002, pp. 419–424.

[11] Y. Liu, L. T. Pillegi, and A. J. Strojwas, "Model order-reduction of $rc(l)$ interconnect including variational analysis," in *Proc. IEEE/ACM Design Automation Conf.*, New Orleans, LA, June 1999, pp. 201–206.

[12] J. W. Demmel, *Applied Numerical Linear Algebra*. Philadelphia, PA: SIAM, 1997.

[13] A. Cangellaris and A. Reuhli, "Model order reduction techniques applied to electromagnetic problems," in *Proc. IEEE Topical Electrical Performance on Electronic Packaging Meeting*, Oct. 2000, pp. 239–242.

Pavan K. Gunupudi (S'98–M'03) received the B.Tech. degree from the Indian Institute of Technology, Chennai, India, in 1997, and the Ph.D. degree from Carleton University, Ottawa, ON, Canada, in 2002.

He is currently an Assistant Professor with the Department of Electronics, Carleton University. His research interests include circuit simulation, computer-aided design of very large scale integration (VLSI) circuits, modeling and simulation of high-speed interconnects and simulation of linear and nonlinear circuits, microelectromechanical systems (MEMS), and opto-electronics.

Dr. Gunupudi was the recipient of numerous academic awards and scholarships including the Indira Gandhi Memorial Fellowship (1998–1999), the Ontario Graduate Scholarship, and the University Medal at Carleton University for outstanding work at the doctoral level. He was also the recipient of the 1998 and 2001 Best Student Paper Award presented at the Electrical Performance of Electronic Packaging Conference.

Roni Khazaka (S'92–M'03) received the Bachelor, Master, and Ph.D. degrees in electrical engineering from Carleton University, Ottawa, ON, Canada in 1995, 1998, and 2002, respectively.

He is currently an Assistant Professor with the Department of Electrical and Computer Engineering, McGill University, Montreal, QC, Canada. He has authored several papers on the simulation of high-speed interconnects and RF circuits. His current research interests include electronic design automation, numerical algorithms and techniques, and the analysis and simulation of RF ICs, high-speed interconnects, and optical networks.

Dr. Khazaka was the IEEE Region 7 (Canada) student representative on the IEEE Student Activities Committee from 1995 to 1998. He served on the IEEE Region 7 Council and contributed to local section and student branch activities. He also served on several IEEE committees. His academic awards and scholarships include the 2002 IEEE Microwave Theory and Techniques Society (IEEE MTT–S) Microwave Prize, the Natural Sciences and Engineering Research Council (NSERC) of Canada Scholarships (at the masters and doctoral levels), Carleton University's Senate Medal and University Medal in Engineering, the Nortel Networks Scholarship, and the IBM Cooperative Fellowship. He was also the recipient of the 2001 Japan Foundation Study Tour Award for outstanding students of the Japanese language, and the Embassy of Japan's Japanese Speech Contest in Ottawa (1998).

Michel S. Nakhla (F'98) received the M.A.Sc. and Ph.D. degrees in electrical engineering from University of Waterloo, ON, Canada, in 1973 and 1975, respectively.

He is currently Chancellor's Professor of Electrical Engineering at Carleton University, Ottawa, ON, Canada. From 1976 to 1988, he was with Bell-Northern Research, Ottawa, ON, Canada, as the Senior Manager of the Computer-Aided Engineering Group. In 1988, he joined Carleton University, as a Professor and the Holder of the Computer-Aided Engineering Senior Industrial Chair established by Bell-Northern Research and the Natural Sciences and Engineering Research Council (NSERC) of Canada. He is the founder of the High-Speed Computer-Aided Design (CAD) Research Group, Carleton University. He serves as a technical consultant for several industrial organizations and is the principal investigator for several major sponsored research projects. His research interests include CAD of VLSI and microwave circuits, modeling and simulation of high-speed interconnects, nonlinear circuits, multidisciplinary optimization, thermal and electromagnetic emission analysis, MEMS, and neural networks. He is an Associate Editor of the *Circuits, Systems and Signal Processing Journal*.

Dr. Nakhla is a frequent invited speaker on the topic of high-speed interconnects. He has been a guest editor for the IEEE TRANSACTIONS ON COMPONENTS, PACKAGING AND MANUFACTURING TECHNOLOGY (Advanced Packaging) and the IEEE TRANSACTIONS ON CIRCUITS AND SYSTEMS—PART II: ANALOG AND DIGITAL SIGNAL PROCESSING. He is currently associate editor of the IEEE TRANSACTIONS ON CIRCUITS AND SYSTEMS—PART I: FUNDAMENTAL THEORY AND APPLICATIONS. He was the corecipient of the IEEE 2002 Microwave Prize in recognition of the most significant contribution by a published paper to the field of interest to the IEEE Microwave Theory and Techniques Society (IEEE MTT-S).

Tom Smy received the B.Sc. and Ph.D. degrees in electrical engineering from the University of Alberta, Edmonton, AB, Canada, in 1986 and 1990, respectively.

He is currently a Professor with the Department of Electronics, Carleton University, Ottawa, ON, Canada. His current research interests include study and simulation of thin-film growth and microstructures, thermal modeling of semiconductor devices and packages, and a variety of back-end processing projects. He has authored or coauthored over 70 journal papers. He also coauthored the SIMBAD and 3D-Films thin-film process simulator.

Dritan Celo received the M.A.Sc. degree in electrical engineering from Carleton University, Ottawa, ON, Canada, in 2001.

From 1986 to 1998, he was an Electrical Engineer with the Research Center for Scientific and Technical Information, Tirana, Albania, Institute of Energy, Tirana, Albania, and the Albanian Power Corporation, Tirana, Albania. Since 2001, he has been a Research Engineer with the Group of Solid State Devices and Integrated Circuit Technology, Department of Electronics, Carleton University. His current research interests include thermal modeling, simulation, and characterization of semiconductor devices, IC components and packages, and CAD. He is currently involved with thermal modeling of electronic systems, particularly at the component printed circuit board (PCB) level.